

Neutrality of coated holes in the presence of screw dislocation dipoles or circular thermal inclusions

X. WANG¹⁾, P. SCHIAVONE²⁾

¹⁾*School of Mechanical and Power Engineering
East China University of Science and Technology
130 Meilong Road, Shanghai 200237, China
e-mail: xuwang@ecust.edu.cn*

²⁾*Department of Mechanical Engineering
University of Alberta
10-203 Donadeo Innovation Centre for Engineering
Edmonton, Alberta Canada T6G 1H9
e-mail: p.schiavone@ualberta.ca*

IN THIS PAPER, WE CONSIDER THE DESIGN OF NEUTRAL COATED HOLES in two particular cases when the thick coating itself is altered by the presence of some form of material imperfection. In the first case we consider anti-plane deformations of a linearly elastic solid when the thick coating applied to the hole includes a screw dislocation dipole. In the second case, we investigate the design of neutral coated holes in plane elasticity when the thick coating contains a circular thermal inclusion and the surrounding linearly elastic solid is subjected to uniform remote hydrostatic stresses. The design is achieved by constructing particular forms of the conformal mapping function for the coating itself. Several examples are presented to demonstrate the resulting solutions. Our numerical results show that the existence of the screw dislocation dipole or the circular thermal inclusion in the coating exerts a significant influence on the shape of the neutral coated hole.

Key words: neutral holes, thick coating, screw dislocation dipole, thermal inclusion, conformal mapping, anti-plane elasticity, plane elasticity.

Copyright © 2018 by IPPT PAN

1. Introduction

A HOLE INTRODUCED INTO AN ELASTIC BODY will inevitably disturb the body's original stress field and often lead to a stress concentration. MANSFIELD [1] was among the first to recognize the feasibility of designing a reinforced “neutral” hole which eliminates any stress concentrations introduced by the hole and hence does not disturb the original stress field in the uncut body. Relevant studies on the design of neutral holes and neutral inclusions in composite materials are abundant and can be found in [2–14]. The concept of neutral inclusions has also been adapted to the design of cloaking structures [15–17].

In the aforementioned discussions of neutrality in composites, the composites themselves are assumed to be free of the presence of dislocations. The existence of dislocations in solid materials, however, has now been confirmed experimentally [18]. Considerable efforts have been made to associate plastic flow in crystalline solids with motions of dislocations (see for example, [19–23]). It is therefore natural to ask whether it remains possible to design neutral holes or inclusions when dislocations are present in the composite? Furthermore, it has been established that the shape of a neutral hole in an isotropic field (or hydrostatic stress field) is certainly circular [7]. Will this interesting and important result persist if the thick coating reinforcing the hole surrounds a circular thermal inclusion?

In this paper, we indeed address each of the aforementioned questions. We begin with an investigation of the neutrality of coated holes in anti-plane elasticity when a screw dislocation dipole is present in the thick coating itself. Secondly, we address the neutrality of coated holes in plane elasticity when the thick coating contains a circular thermal inclusion and the solid is subjected to uniform remote hydrostatic stresses. Our method includes the introduction of particular forms of the corresponding conformal mapping which includes either a logarithmic function to account for the existence of the dislocation dipole or a first-order pole in the case of the circular thermal inclusion. These conformal mappings are then the key to the successful solution of the corresponding boundary value problems. We validate and illustrate our solutions via the use of several numerical examples.

2. Complex variable formulation

Under anti-plane shear deformations of a linearly isotropic elastic material, in a Cartesian coordinate system, the two shear stress components σ_{31} and σ_{32} , the out-of-plane displacement w and the stress function φ can be expressed in terms of a single analytic function $f(z)$ of the complex variable $z = x_1 + ix_2$ as [24]

$$(2.1) \quad \sigma_{32} + i\sigma_{31} = \mu f'(z), \quad \varphi + i\mu w = \mu f(z),$$

where μ is the shear modulus and the two stress components can be expressed in terms of the same stress function as [24]

$$(2.2) \quad \sigma_{32} = \varphi_{,1}, \quad \sigma_{31} = -\varphi_{,2}.$$

For plane deformations of an isotropic elastic material, the stresses $(\sigma_{11}, \sigma_{22}, \sigma_{12})$, displacements (u_1, u_2) and stress functions (φ_1, φ_2) can be expressed in terms of two analytic functions $\phi(z)$ and $\psi(z)$ of the complex variable $z = x_1 + ix_2$ as [25]

$$\begin{aligned}
 (2.3) \quad & \sigma_{11} + \sigma_{22} = 2[\phi'(z) + \overline{\phi'(z)}], \\
 & \sigma_{22} - \sigma_{11} + 2i\sigma_{12} = 2[\bar{z}\phi''(z) + \psi'(z)], \\
 (2.4) \quad & 2\mu(u_1 + iu_2) = \kappa\phi(z) - z\overline{\phi'(z)} - \overline{\psi(z)}, \\
 & \varphi_1 + i\varphi_2 = i[\phi(z) + z\overline{\phi'(z)} + \overline{\psi(z)}],
 \end{aligned}$$

where $\kappa = 3 - 4\nu$ for plane strain and $\kappa = (3 - \nu)/(1 + \nu)$ for plane stress with ν ($0 \leq \nu \leq 1/2$) being the Poisson's ratio. In addition, the stresses are related to the stress functions through [24]

$$\begin{aligned}
 (2.5) \quad & \sigma_{11} = -\varphi_{1,2}, \quad \sigma_{12} = \varphi_{1,1}, \\
 & \sigma_{21} = -\varphi_{2,2}, \quad \sigma_{22} = \varphi_{2,1}.
 \end{aligned}$$

3. Neutral coated holes in the presence of screw dislocation dipoles

Consider a domain in \mathbb{R}^2 , infinite in extent, containing a hole occupying a simply connected region Ω , as shown in Fig. 1. The hole is surrounded by a thick coating occupying a doubly connected region S_2 and the coating is perfectly bonded to the surrounding matrix occupying the region S_1 . The coating-matrix interface is denoted by L_1 whilst the traction-free boundary of the hole

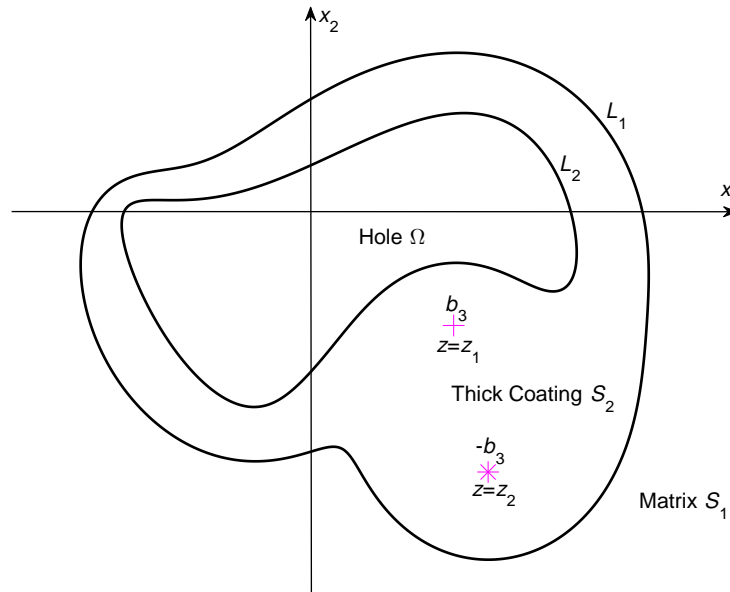


FIG. 1. A neutral coated hole in the presence of a screw dislocation dipole in the thick coating.

is denoted by L_2 . The matrix is subjected to uniform remote anti-plane shear stresses $(\sigma_{31}^\infty, \sigma_{32}^\infty)$ while the coating is under the action of a screw dislocation dipole composed of a screw dislocation with the Burgers vector b_3 located at $z = z_1$ and a second screw dislocation with the opposite Burgers vector $-b_3$ located at $z = z_2$ (see Fig. 1). Throughout the paper, the subscripts 1 and 2 are used to identify the respective quantities in S_1 and S_2 . Our objective is to design the shape of the thick coating to achieve neutrality, i.e. to ensure that the coated hole will not disturb the original uniform stress field in the surrounding matrix. The incorporation of a dislocation dipole as opposed to a dislocation in the coating is to ensure the single-valuedness of the displacement field on any contour in the matrix surrounding the coating.

The boundary value problem for the two-phase composite takes the following form:

$$(3.1a) \quad \begin{aligned} f_2(z) + \overline{f_2(z)} &= \Gamma f_1(z) + \Gamma \overline{f_1(z)}, \\ f_2(z) - \overline{f_2(z)} &= f_1(z) - \overline{f_1(z)}, \quad z \in L_1; \end{aligned}$$

$$(3.1b) \quad f_2(z) + \overline{f_2(z)} = 0, \quad z \in L_2;$$

$$(3.1c) \quad \begin{aligned} f_2(z) &\cong \frac{b_3}{2\pi} \ln(z - z_1) + O(1), \quad z \rightarrow z_1, \\ f_2(z) &\cong -\frac{b_3}{2\pi} \ln(z - z_2) + O(1), \quad z \rightarrow z_2; \end{aligned}$$

$$(3.1d) \quad f_1(z) = Cz, \quad z \in S_1,$$

where $\Gamma = \mu_1/\mu_2$ and the complex number C is given by

$$(3.2) \quad C = \frac{\sigma_{32}^\infty + i\sigma_{31}^\infty}{\mu_1}.$$

Consider the following conformal mapping function for the coating

$$(3.3) \quad \begin{aligned} z &= \omega(\xi) \\ &= q \ln \frac{\xi - \bar{\xi}_1^{-1}}{\xi - \bar{\xi}_2^{-1}} + \sum_{n=1}^{+\infty} (a_n \xi^n + a_{-n} \xi^{-n}), \quad \xi = \omega^{-1}(z), \quad r \leq |\xi| \leq 1, \end{aligned}$$

where q , a_n , a_{-n} , $n = 1, 2, \dots, +\infty$ are complex constants to be determined, $\xi_1 = \omega^{-1}(z_1)$ and $\xi_2 = \omega^{-1}(z_2)$. Using the mapping function, the coating in the z -plane is mapped onto an annulus $r \leq |\xi| \leq 1$ in the ξ -plane, the coating-matrix interface L_1 in the z -plane is mapped onto $|\xi| = 1$ in the ξ -plane, the traction-free boundary of the hole L_2 in the z -plane is mapped onto $|\xi| = r$ in

the ξ -plane, $z = z_1$ is mapped onto $\xi = \xi_1$ and $z = z_2$ is mapped onto $\xi = \xi_2$ (see Fig. 2). The appearance of the logarithmic function $\ln \frac{\xi - \bar{\xi}_1^{-1}}{\xi - \bar{\xi}_2^{-1}}$ in the mapping function is to account for the existence of the screw dislocation dipole.

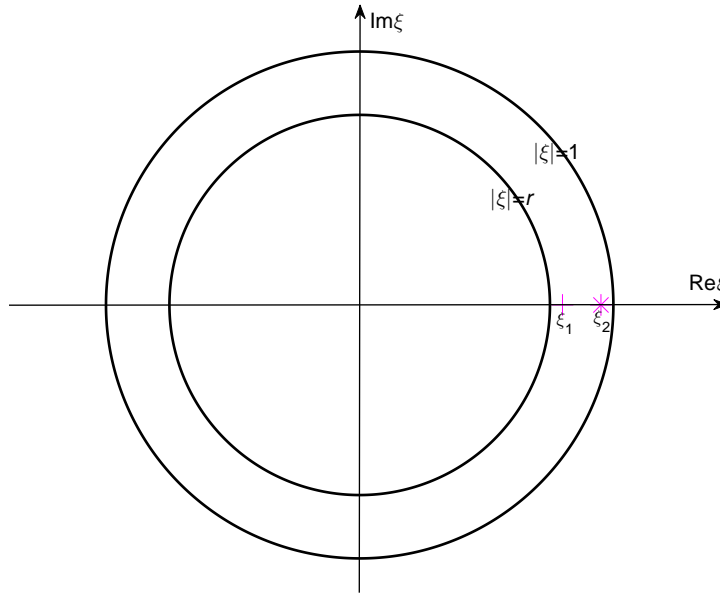


FIG. 2. The problem in the ξ -plane.

By enforcing the continuity conditions of traction and displacement across the coating-matrix interface L_1 in Eq. (3.1a), we arrive at

$$(3.4) \quad f_2(\xi) = f_2(\omega(\xi)) = \frac{C(\Gamma + 1)}{2} \omega(\xi) + \frac{\bar{C}(\Gamma - 1)}{2} \bar{\omega}\left(\frac{1}{\xi}\right), \quad r \leq |\xi| \leq 1,$$

or more explicitly

$$(3.5) \quad f_2(\xi) = f_2(\omega(\xi)) = \frac{C(\Gamma + 1)}{2} \left[q \ln \frac{\xi - \bar{\xi}_1^{-1}}{\xi - \bar{\xi}_2^{-1}} + \sum_{n=1}^{+\infty} (a_n \xi^n + a_{-n} \xi^{-n}) \right] + \frac{\bar{C}(\Gamma - 1)}{2} \left[\bar{q} \ln \frac{\xi - \xi_1}{\xi - \xi_2} + \sum_{n=1}^{+\infty} (\bar{a}_n \xi^{-n} + \bar{a}_{-n} \xi^n) \right], \quad r \leq |\xi| \leq 1.$$

By enforcing the traction-free condition along the hole boundary L_2 in Eq. (3.1b),

the following relationships can be obtained

$$(3.6) \quad a_{-n} = \frac{\bar{C}[1 - \Gamma - r^{2n}(\Gamma + 1)]}{C[\Gamma + 1 + r^{2n}(\Gamma - 1)]} \bar{a}_n + \frac{r^{2n} \left[\frac{\bar{C}}{C} \bar{q}(\Gamma + 1)(\xi_1^n - \xi_2^n) + q(\Gamma - 1)(\bar{\xi}_1^{-n} - \bar{\xi}_2^{-n}) \right]}{n[\Gamma + 1 + r^{2n}(\Gamma - 1)]}, \quad n = 1, 2, \dots, +\infty,$$

which demonstrates that a_{-n} is related to a_n . It can be easily checked that in the absence of the screw dislocation dipole with $q = 0$, Eq. (3.6) simply reduces to the result by MILTON and SERKOV [8].

A comparison of Eq. (3.5) with Eq. (3.1c) leads to

$$(3.7) \quad q = \frac{b_3}{\pi C(\Gamma - 1)},$$

which indicates that q is real if C is real (i.e., $\sigma_{32}^\infty \neq 0$, $\sigma_{31}^\infty = 0$), and q is purely imaginary if C is purely imaginary (i.e., $\sigma_{31}^\infty \neq 0$, $\sigma_{32}^\infty = 0$).

Examples of neutral coated holes are constructed in Figs. 3 and 4 with only $a_1 \neq 0$ in Eq. (3.6); in Figs. 5 and 6 with only $a_1, a_2 \neq 0$; in Figs. 7 and 8 with only $a_1, a_3 \neq 0$ in Eq. (3.6); in Figs. 9 and 10 with only $a_1, a_4 \neq 0$ in Eq. (3.6); in Fig. 11 with only $a_1, a_5 \neq 0$ in Eq. (3.6); and in Fig. 12 with only $a_1, a_6 \neq 0$

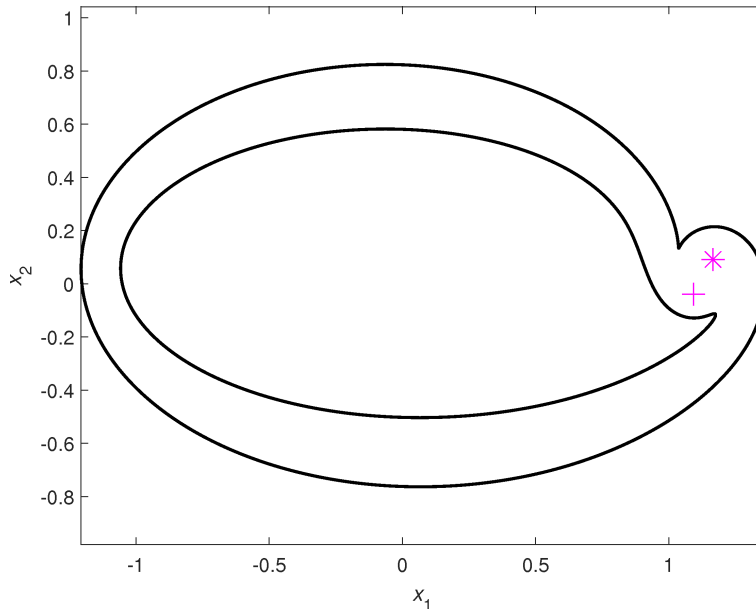


FIG. 3. Neutral coated hole when choosing $\text{Re } C = 0$, $\Gamma = 1/3$, $r = 0.8$, $a_1 = 1$, $q = 0.25i$, $\xi_1 = 0.85$, $\xi_2 = 0.95$.

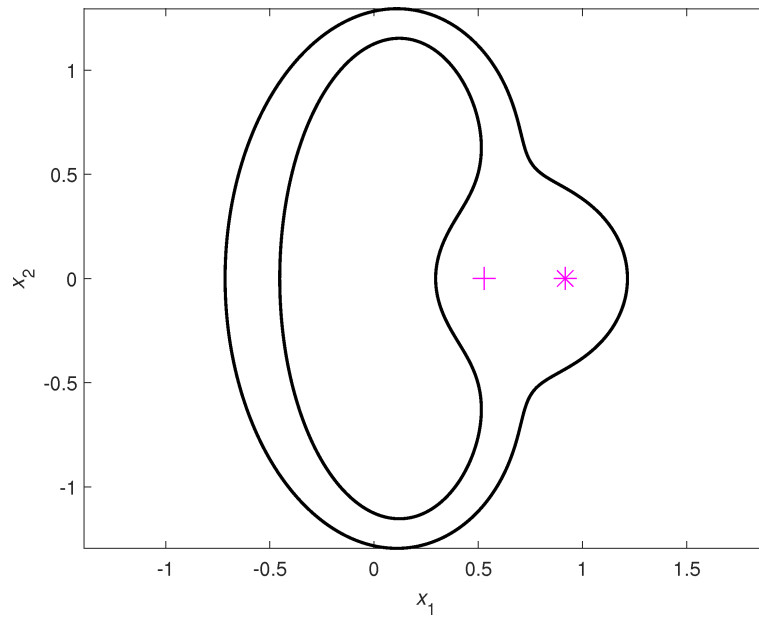


FIG. 4. Neutral coated hole when choosing $\text{Im } C = 0$, $\Gamma = 1/3$, $r = 0.8$, $a_1 = 1$, $q = 0.5$, $\xi_1 = 0.85$, $\xi_2 = 0.95$.

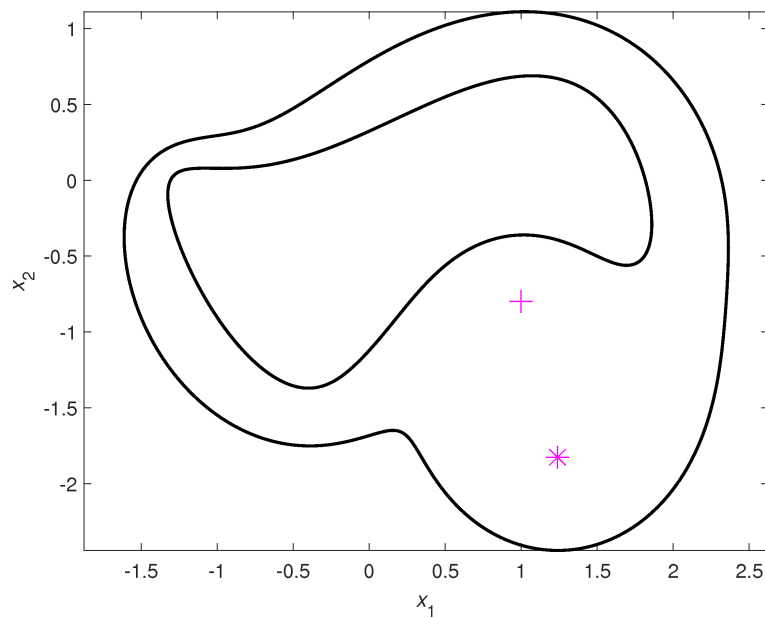


FIG. 5. Neutral coated hole when choosing $\text{Re } C = 0$, $\Gamma = 1/3$, $r = 0.75$, $a_1 = 1 - i$, $a_2 = 0.3 - 0.3i$, $q = -i$, $\xi_1 = 0.8$, $\xi_2 = 0.95$.

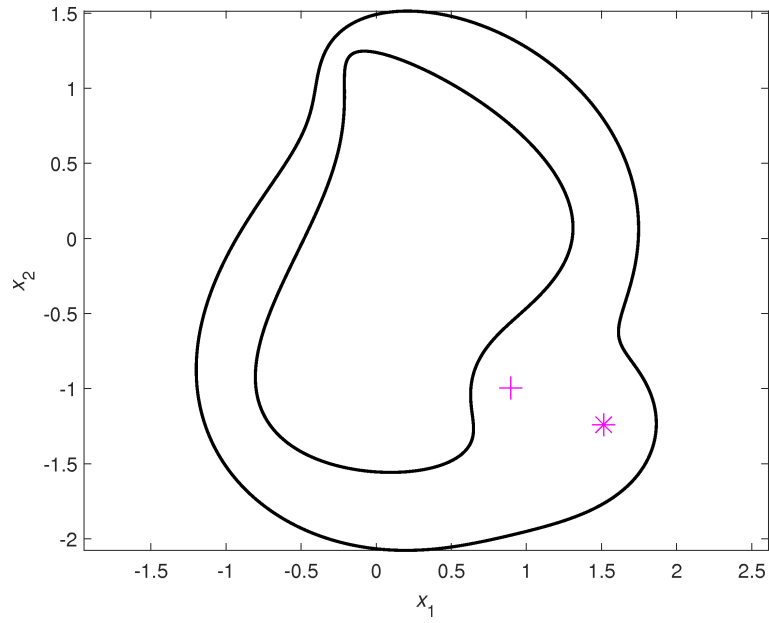


FIG. 6. Neutral coated hole when choosing $\text{Im } C = 0$, $\Gamma = 1/3$, $r = 0.75$, $a_1 = 1 - i$, $a_2 = 0.3 - 0.3i$, $q = 0.5$, $\xi_1 = 0.8$, $\xi_2 = 0.95$.

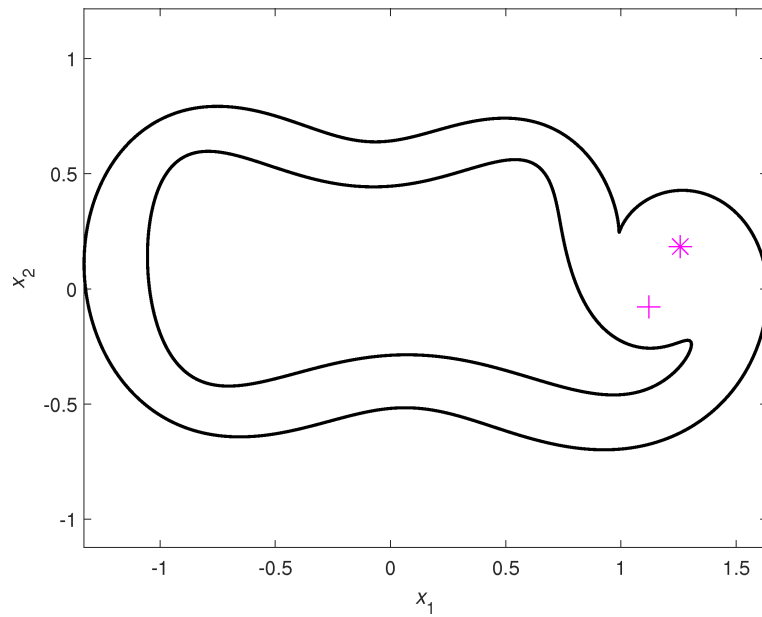


FIG. 7. Neutral coated hole when choosing $\text{Re } C = 0$, $\Gamma = 1/3$, $r = 0.8$, $a_1 = 1$, $a_3 = 0.17$, $q = 0.5i$, $\xi_1 = 0.85$, $\xi_2 = 0.95$.

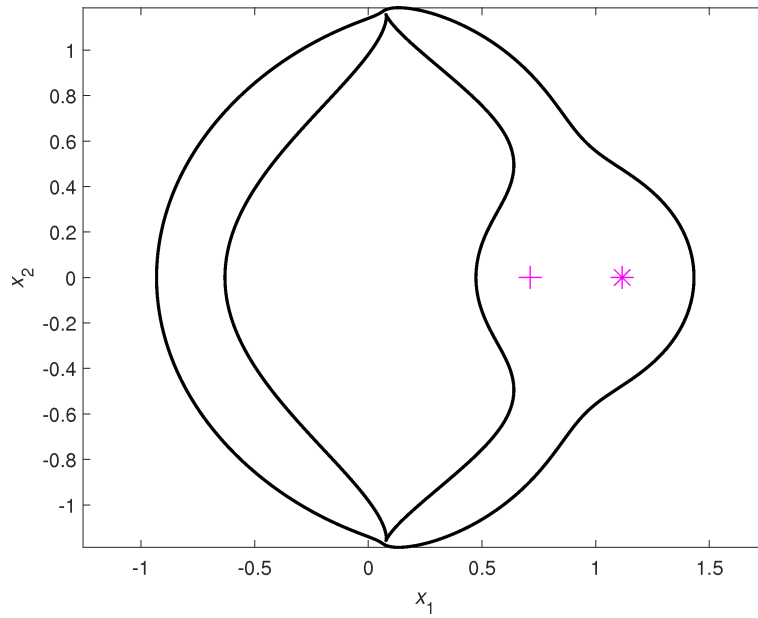


FIG. 8. Neutral coated hole when choosing $\text{Im } C = 0$, $\Gamma = 1/3$, $r = 0.8$, $a_1 = 1$, $a_3 = 0.17$, $q = 0.5$, $\xi_1 = 0.85$, $\xi_2 = 0.95$.

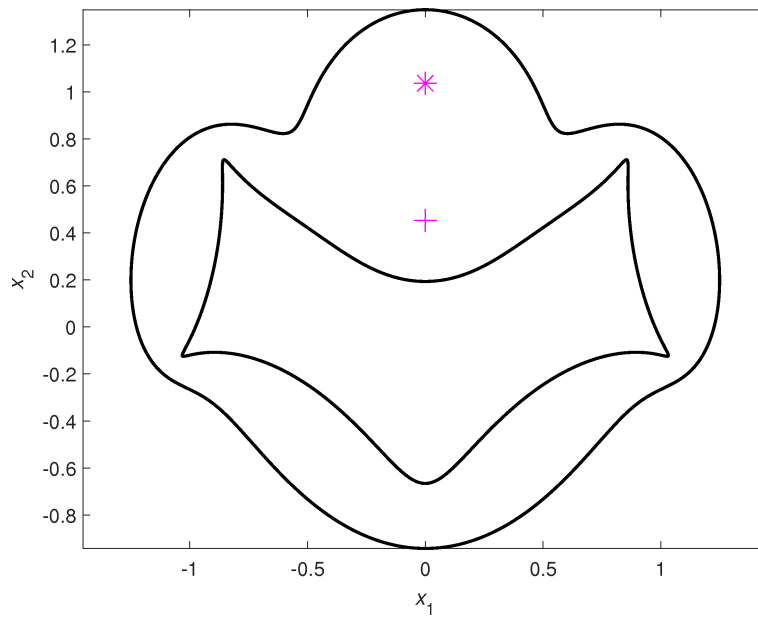


FIG. 9. Neutral coated hole when choosing $\text{Re } C = 0$, $\Gamma = 1/3$, $r = 0.75$, $a_1 = i$, $a_3 = -0.1i$, $q = 0.5i$, $\xi_1 = 0.8$, $\xi_2 = 0.95$.

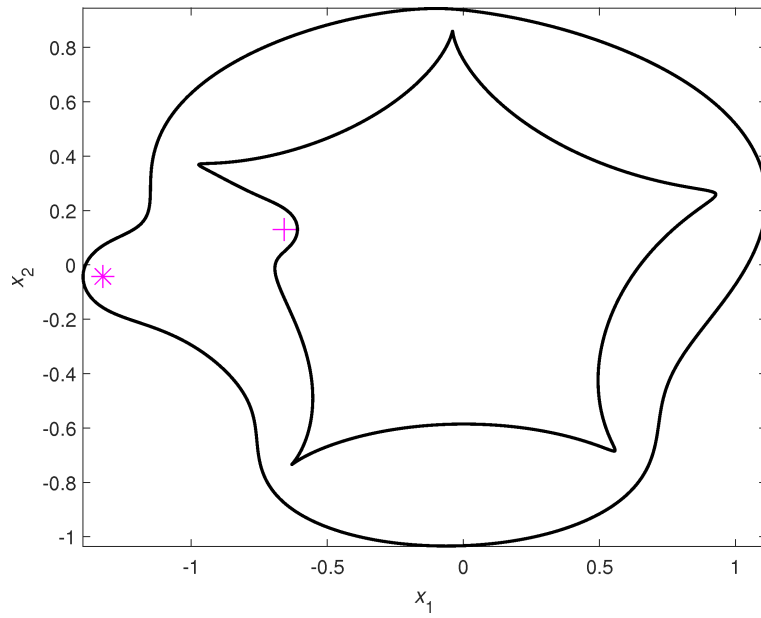


FIG. 10. Neutral coated hole when choosing $\text{Im } C = 0$, $\Gamma = 1/4$, $r = 0.75$, $a_1 = i$, $a_3 = -0.1i$, $q = -0.1$, $\xi_1 = 0.755i$, $\xi_2 = 0.995i$.

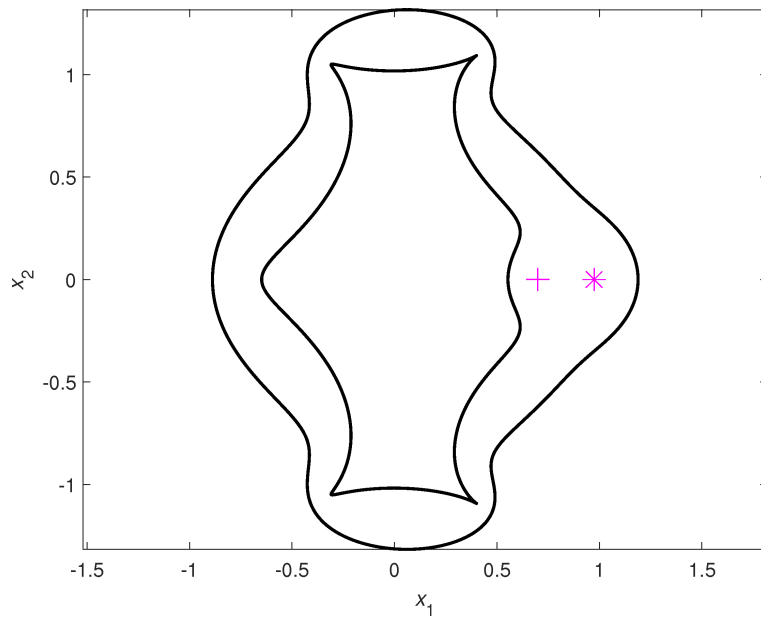


FIG. 11. Neutral coated hole when choosing $\text{Im } C = 0$, $\Gamma = 1/3$, $r = 0.8$, $a_1 = 1$, $a_5 = 0.1$, $q = 0.3$, $\xi_1 = 0.85$, $\xi_2 = 0.95$.

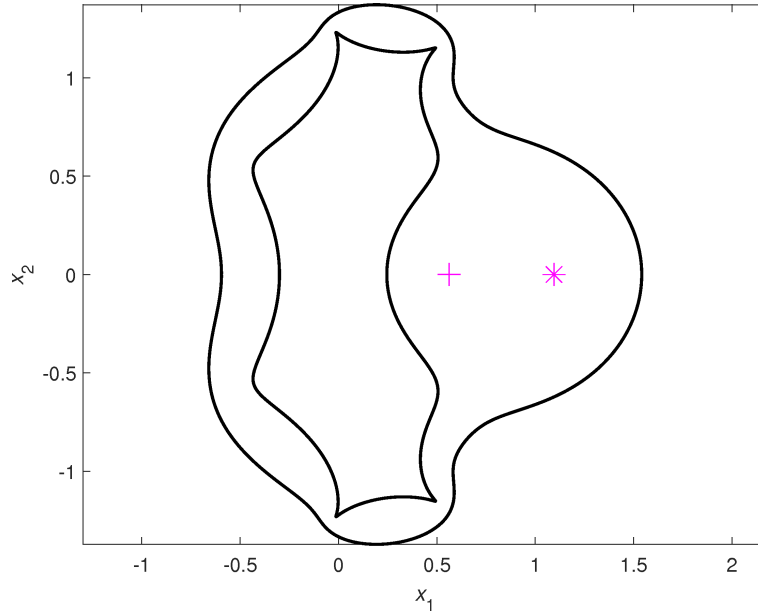


FIG. 12. Neutral coated hole when choosing $\text{Im} C = 0$, $\Gamma = 1/3$, $r = 0.8$, $a_1 = 1$, $a_6 = 0.05$, $q = 0.8$, $\xi_1 = 0.85$, $\xi_2 = 0.95$.

in Eq. (3.6). The values of a_n and r in Figs. 5–10 are those adopted by MILTON and SERKOV [8] in the absence of the screw dislocation dipole. In all of these figures, the plus sign “+” indicates the position of the screw dislocation at $z = z_1$ whilst the star “*” indicates that of the other screw dislocation with the opposite Burgers vector at $z = z_2$. It is observed from Figs. 3 and 4 that the neutral coated hole is no longer a confocal ellipse construction [26, 27] when a screw dislocation dipole is present in the coating although only a_1 is nonzero in Eq. (3.6). By comparing Fig. 5 with Fig. 1c in [8], Fig. 7 with Fig. 2b in [8], Fig. 9 with Fig. 3c in [8], one can conclude that the existence of the screw dislocation dipole in the thick coating will significantly alter the shapes of the neutral coated holes, especially those portions in the neighborhood of the screw dislocation dipole. As the index n of the nonzero coefficient a_n increases, the shape of the coated hole becomes more complicated (see Figs. 11 and 12).

We show in Fig. 13 neutral coated holes which are symmetric with respect to both the x_1 - and x_2 -axes. The positions of the two screw dislocations comprising the screw dislocation dipole are also symmetric with respect to the x_2 -axis. It is seen that the outer boundary of the thick coating has been significantly influenced by the nearby screw dislocation dipole. In all the neutral coated holes shown in Figs. 3–13, the coating is always stiffer than the surrounding matrix (i.e., $\Gamma < 1$) in order to achieve neutrality.

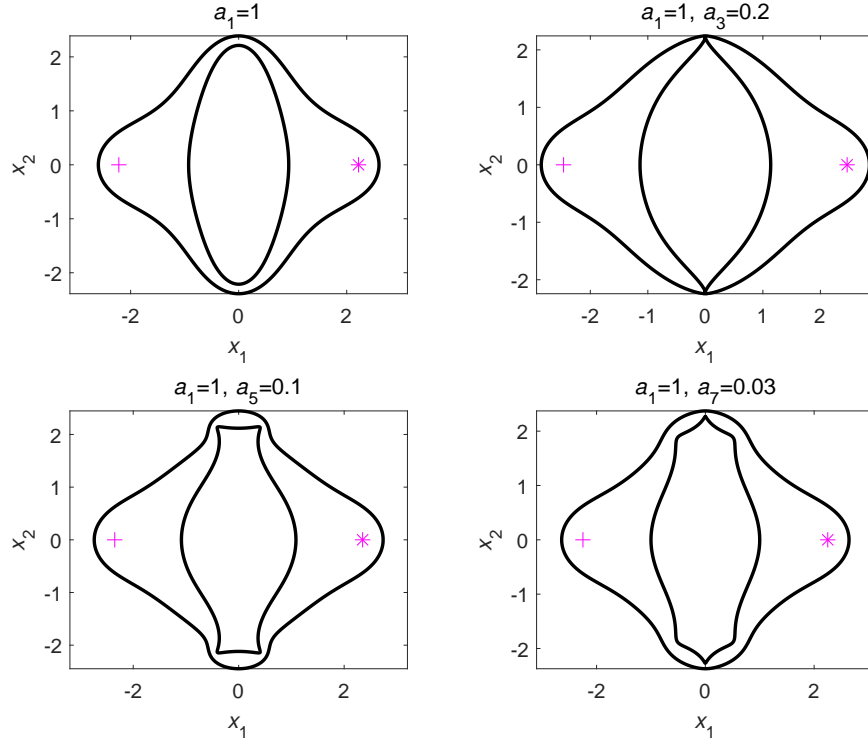


FIG. 13. Neutral coated holes when choosing $\text{Im } C = 0$, $\Gamma = 1/3$, $r = 0.8$, $q = 0.5$, $\xi_1 = -0.98$, $\xi_2 = 0.98$. In addition, $a_1 = 1$ or $a_1 = 1, a_3 = 0.2$ or $a_1 = 1, a_5 = 0.1$ or $a_1 = 1, a_7 = 0.03$ in Eq. (3.6).

4. Neutral coated holes in the presence of circular thermal inclusions

As shown in Fig. 14, we consider a domain in \mathbb{R}^2 , infinite in extent, containing a hole occupying a simply connected region Ω . The hole is surrounded by a thick coating occupying a doubly connected region S_2 with the coating assumed to be perfectly bonded to the surrounding matrix occupying the region S_1 . The region occupying the coating-matrix interface is denoted by L_1 whilst the traction-free boundary of the hole is denoted by L_2 . The matrix is subjected to uniform remote hydrostatic stresses $\sigma_{11}^\infty = \sigma_{22}^\infty = \sigma^0$, $\sigma_{12}^\infty = 0$. In addition, a circular region $|z - z_0| \leq R$ in the coating undergoes uniform stress-free eigenstrains $\varepsilon_{11}^* = \varepsilon_{22}^* = \varepsilon^*$, $\varepsilon_{12}^* = 0$. We again adopt the convention that the subscripts 1 and 2 identify the respective quantities in S_1 and S_2 . Our objective is to design the shape of the thick coating such that the coated hole will not disturb the original uniform hydrostatic stress field in the surrounding matrix.

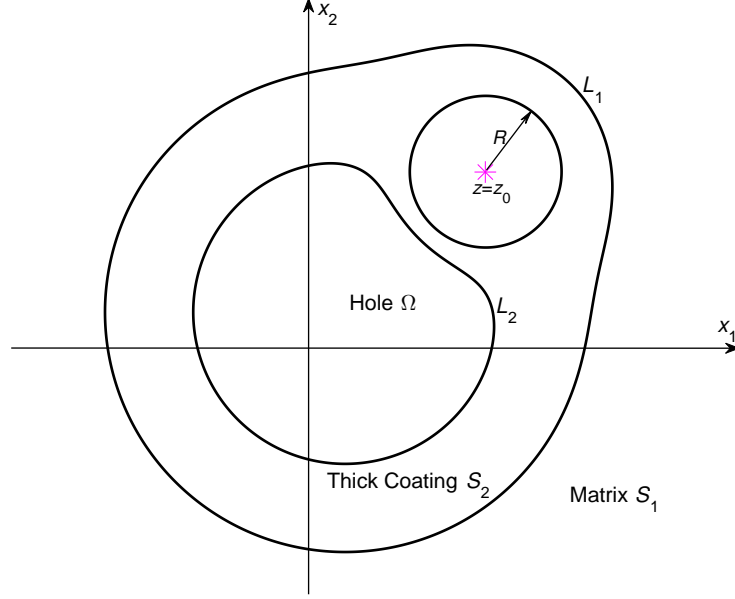


FIG. 14. A neutral coated hole with a circular thermal inclusion in the coating.

The boundary value problem for the two-phase composite takes the following form:

$$(4.1a) \quad \begin{aligned} \phi_2(z) + z\overline{\phi_2'(z)} + \overline{\psi_2(z)} &= \phi_1(z) + z\overline{\phi_1'(z)} + \overline{\psi_1(z)}, \\ \kappa_2\phi_2(z) - z\overline{\phi_2'(z)} - \overline{\psi_2(z)} &= \Gamma\kappa_1\phi_1(z) - \Gamma z\overline{\phi_1'(z)} - \Gamma\overline{\psi_1(z)}, \quad z \in L_1; \end{aligned}$$

$$(4.1b) \quad \phi_2(z) + z\overline{\phi_2'(z)} + \overline{\psi_2(z)} = 0, \quad z \in L_2;$$

$$(4.1c) \quad \phi_2(z) \cong O(1), \quad \psi_2(z) \cong -\frac{4\mu_2\varepsilon^*}{1+\kappa_2} \frac{R^2}{z-z_0} + O(1), \quad z \rightarrow z_0;$$

$$(4.1d) \quad \phi_1(z) = Az, \quad \psi_1(z) = 0, \quad z \in S_1,$$

where $\Gamma = \mu_2/\mu_1$, and the real constant A is related to remote loading through

$$(4.2) \quad A = \frac{\sigma_{11}^\infty + \sigma_{22}^\infty}{4} = \frac{\sigma^0}{2}.$$

In writing the asymptotic behavior in Eq. (4.1c), we have used the result given by SUO [28] and RU [29]. A detailed explanation of Eq. (4.1c) is given in the Appendix. We emphasize that the definition of Γ used here for plane elasticity differs from that used in the case anti-plane elasticity discussed in the previous section.

Consider the following conformal mapping function for the thick coating

$$(4.3) \quad z = \omega(\xi) = \frac{q}{\xi - \bar{\xi}_0^{-1}} + \sum_{n=1}^{+\infty} (a_n \xi^n + a_{-n} \xi^{-n}), \quad \xi = \omega^{-1}(z), \quad r \leq |\xi| \leq 1,$$

where q is a complex constant, $a_n, a_{-n}, n = 1, 2, \dots, +\infty$ are unknown complex constants to be determined and $\xi_0 = \omega^{-1}(z_0)$. Using the mapping function in Eq. (4.3), the thick coating in the z -plane is mapped onto an annulus $r \leq |\xi| \leq 1$ in the ξ -plane, the coating-matrix interface L_1 in the z -plane is mapped onto $|\xi| = 1$ in the ξ -plane, the traction-free boundary of the hole L_2 in the z -plane is mapped onto $|\xi| = r$ in the ξ -plane and the point $z = z_0$ is mapped onto $\xi = \xi_0$ (see Fig. 15). The appearance in Eq. (4.3) of the first-order pole at $\xi = \bar{\xi}_0^{-1}$ outside the annulus is to account for the existence of the circular thermal inclusion in the thick coating.

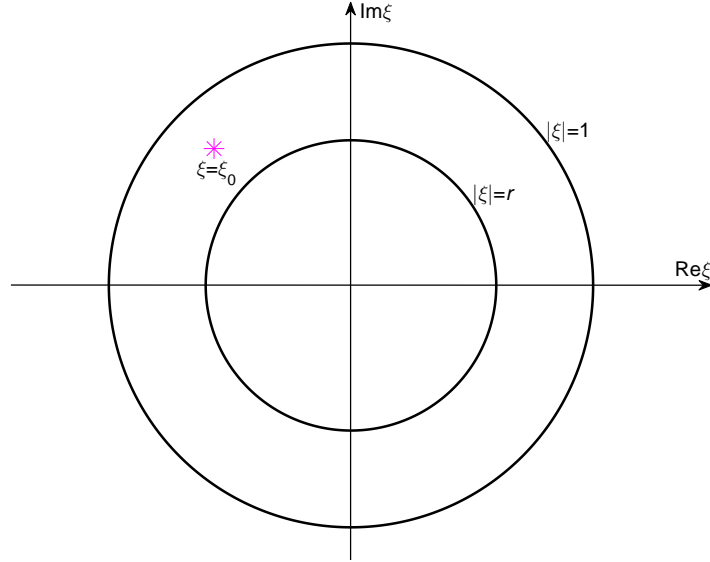


FIG. 15. The problem in the image ξ -plane.

By enforcing the continuity conditions of displacement and traction across the coating-matrix interface L_1 (Eq. (4.1a)) we arrive at

$$(4.4) \quad \begin{aligned} \phi_2(\xi) = \phi_2(\omega(\xi)) &= \frac{A[\Gamma(\kappa_1 - 1) + 2]}{\kappa_2 + 1} \left[\frac{q}{\xi - \bar{\xi}_0^{-1}} + \sum_{n=1}^{+\infty} (a_n \xi^n + a_{-n} \xi^{-n}) \right], \\ \psi_2(\xi) = \psi_2(\omega(\xi)) &= \frac{2A[\kappa_2 - 1 - \Gamma(\kappa_1 - 1)]}{\kappa_2 + 1} \\ &\quad \times \left[-\frac{\bar{q}\xi_0^2}{\xi - \xi_0} + \sum_{n=1}^{+\infty} (\bar{a}_n \xi^{-n} + \bar{a}_{-n} \xi^n) \right], \quad r \leq |\xi| \leq 1. \end{aligned}$$

The traction-free boundary condition along the hole boundary L_2 (Eq. (4.1b)) allows us to determine the complex coefficients a_n , a_{-n} , $n = 1, 2, \dots, +\infty$ uniquely as follows

$$(4.5) \quad a_n = \frac{q\bar{\xi}_0^{n+1}}{1 + \beta r^{-2n}}, \quad a_{-n} = -\frac{q\beta r^{2n}\xi_0^{1-n}}{1 + \beta r^{2n}}, \quad n = 1, 2, \dots, +\infty,$$

where

$$(4.6) \quad \beta = \frac{\kappa_2 - 1 - \Gamma(\kappa_1 - 1)}{\Gamma(\kappa_1 - 1) + 2}.$$

A comparison of Eq. (4.4) with Eq. (4.1c) leads to the following relationship

$$(4.7) \quad q = \frac{4R^2\mu_2\varepsilon^*}{\sigma^0[\kappa_2 - 1 - \Gamma(\kappa_1 - 1)]} \frac{1}{\xi_0^2\omega'(\xi_0)}.$$

Inserting Eq. (4.5) into Eq. (4.3), we obtain the following expression for $\omega'(\xi_0)$:

$$(4.8) \quad \omega'(\xi_0) = -\frac{q\bar{\xi}_0^2}{(|\xi_0|^2 - 1)^2} + q\bar{\xi}_0^2 \sum_{n=1}^{+\infty} n \left(\frac{|\xi_0|^{2n-2}}{1 + \beta r^{-2n}} + \frac{\beta r^{2n}|\xi_0|^{-2n-2}}{1 + \beta r^{2n}} \right).$$

Consequently, $\omega'(\xi_0)$ is uniquely determined from Eq. (4.8) for given values of Γ , κ_1 , κ_2 , r , ξ_0 and q . Accordingly, the ratio $R^2\mu_2\varepsilon^*/\sigma^0$ can be further determined from Eq. (4.7) as follows

$$(4.9) \quad \frac{R^2\mu_2\varepsilon^*}{\sigma^0} = \frac{1}{4}|q|^2|\xi_0|^2[\kappa_2 - 1 - \Gamma(\kappa_1 - 1)] \\ \times \left[-\frac{|\xi_0|^2}{(|\xi_0|^2 - 1)^2} + \sum_{n=1}^{+\infty} n \left(\frac{|\xi_0|^{2n}}{1 + \beta r^{-2n}} + \frac{\beta r^{2n}|\xi_0|^{-2n}}{1 + \beta r^{2n}} \right) \right].$$

Note that the right-hand side of Eq. (4.9) is always real-valued.

In addition, we see from Eqs. (4.2)–(4.4) and the Appendix that the mean stress is uniform in the region S'_2 occupied by the thick coating outside the circular thermal inclusion and is given by

$$(4.10) \quad \sigma_{11} + \sigma_{22} = \frac{2\sigma^0[\Gamma(\kappa_1 - 1) + 2]}{\kappa_2 + 1}, \quad z \in S'_2.$$

It then follows from Eq. (4.10) that the hoop stress is constant along either L_1 or L_2 on the coating side as follows

$$(4.11) \quad \sigma_{tt} = \frac{\sigma^0[2\Gamma(\kappa_1 - 1) + 3 - \kappa_2]}{\kappa_2 + 1}, \quad z \in L_1; \\ \sigma_{tt} = \frac{2\sigma^0[\Gamma(\kappa_1 - 1) + 2]}{\kappa_2 + 1}, \quad z \in L_2.$$

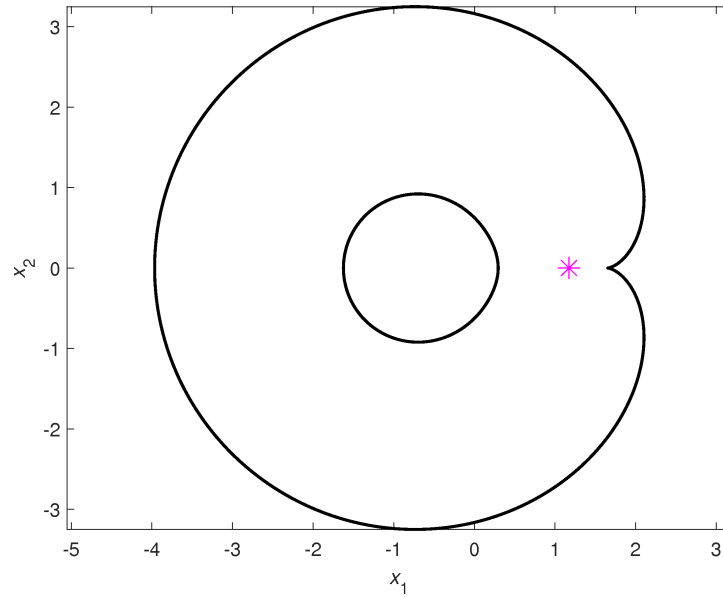


FIG. 16. A neutral coated hole when choosing $\Gamma = 1.2582$, $\kappa_1 = \kappa_2 = 2$, $r = 0.3$, $\xi_0 = 0.65$, $q = 1$.

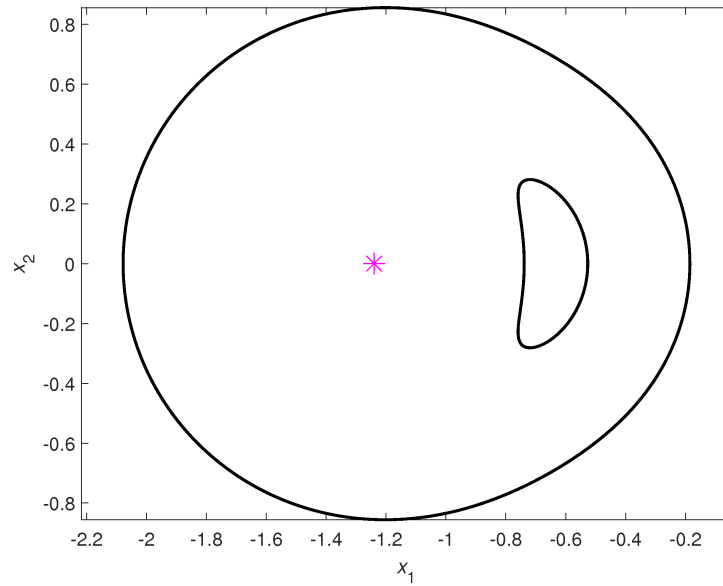


FIG. 17. A neutral coated hole when choosing $\Gamma = 2$, $\kappa_1 = \kappa_2 = 2$, $r = 0.3$, $\xi_0 = 0.65$, $q = 1$.

Thus the “equal strength” design criterion advanced by CHEREPANOV [30] has also been achieved.

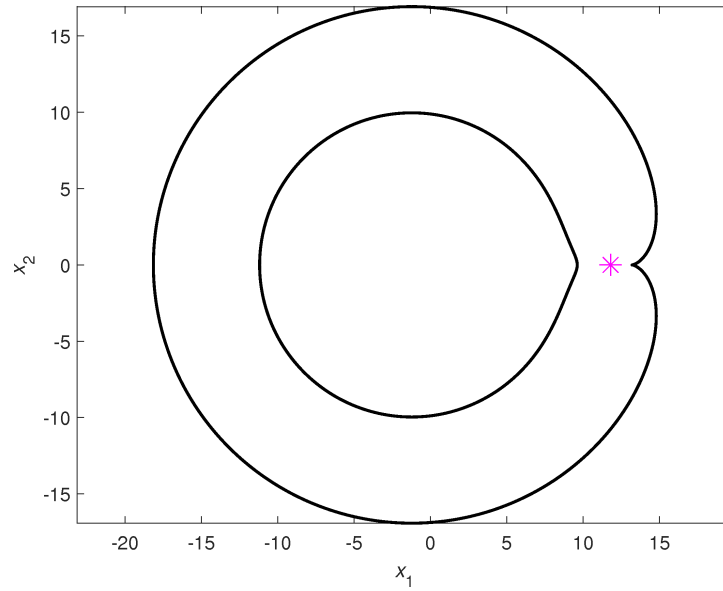


FIG. 18. A neutral coated hole when choosing $\Gamma = 2.5922$, $\kappa_1 = \kappa_2 = 2$, $r = 0.6$, $\xi_0 = 0.8$, $q = 1$.

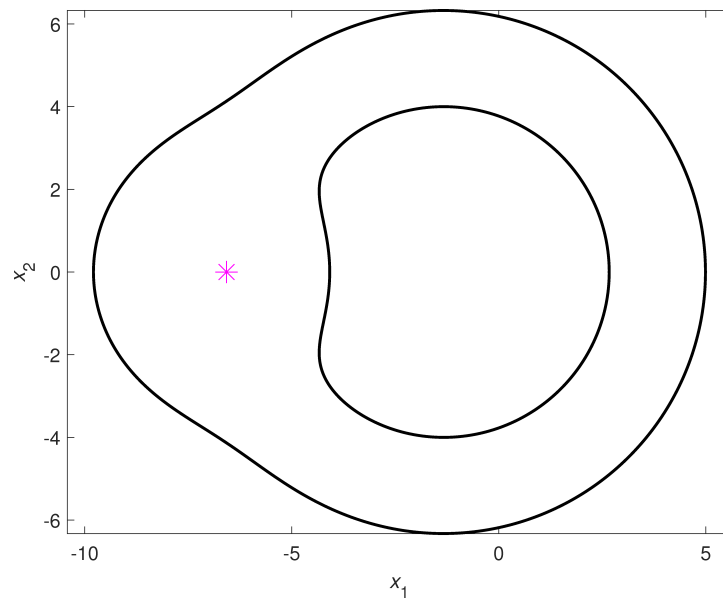


FIG. 19. A neutral coated hole when choosing $\Gamma = 3$, $\kappa_1 = \kappa_2 = 2$, $r = 0.6$, $\xi_0 = 0.8$, $q = 1$.

Illustrated in Figs. 16 to 21 are the resulting neutral coated holes for three typical values of the coating thickness parameter $r = 0.3, 0.6, 0.9$. The star in

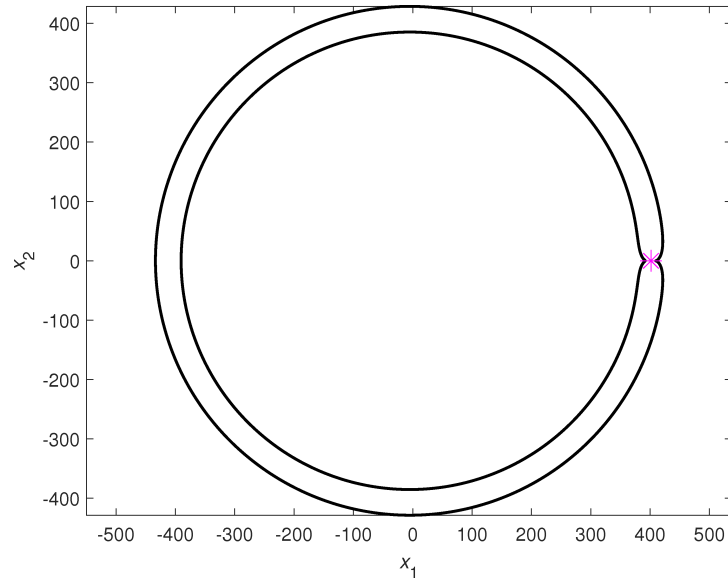


FIG. 20. A neutral coated hole when choosing $\Gamma = 13.6492$, $\kappa_1 = \kappa_2 = 2$, $r = 0.9$, $\xi_0 = 0.95$, $q = 1$.

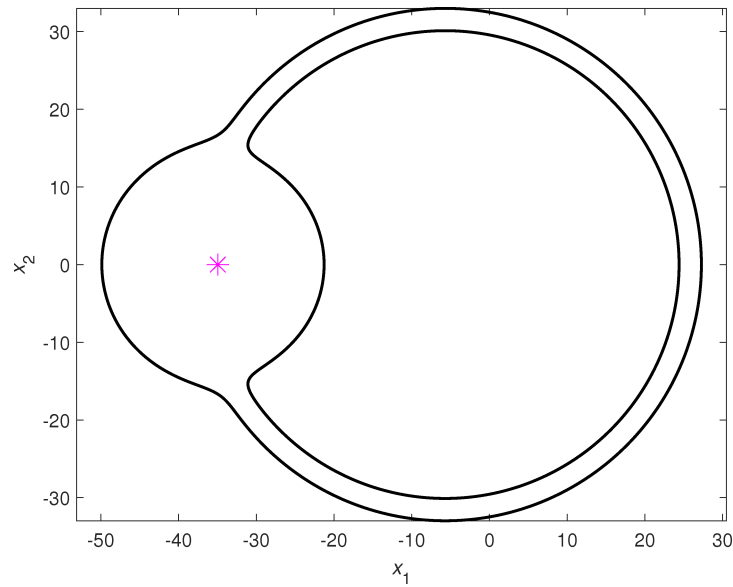


FIG. 21. A neutral coated hole when choosing $\Gamma = 16$, $\kappa_1 = \kappa_2 = 2$, $r = 0.9$, $\xi_0 = 0.95$, $q = 1$.

each figure indicates the position of $z = z_0$, the center of the circular thermal inclusion. In all the six figures, the coating is always stiffer than the surrounding matrix (i.e., $\Gamma > 1$) in order to achieve neutrality. In addition, in Figs. 16 and 18,

the hole boundary L_2 is convex whereas the coating-matrix interface L_1 becomes non-convex and has a sharp corner; in Fig. 17, the coating-matrix interface L_1 is convex whereas the hole boundary L_2 becomes non-convex; in Figs. 19–21, both the coating-matrix interface L_1 and the hole boundary L_2 become non-convex. We observe the general trend that as the value of the parameter r increases, the minimum value of Γ (> 1) must increase in order to ensure that there is no self-intersecting boundary for L_1 and L_2 (see Figs. 16, 18, 20). On the other hand, the value of Γ cannot be set arbitrarily large. The above trend can be more clearly observed in Fig. 22. The pair (r, Γ) must lie between the two curves in Fig. 22. We further note that the results in Fig. 22 are valid for any value of q .

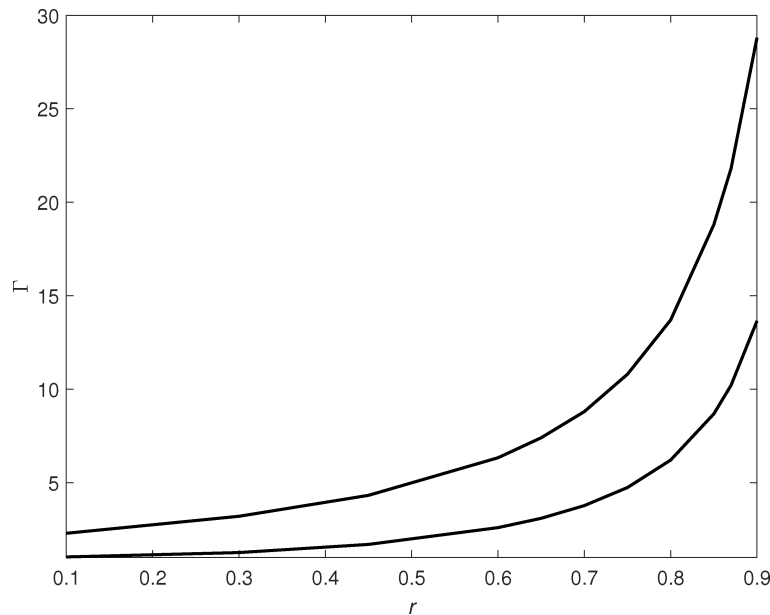


FIG. 22. The range of permissible Γ for different values of the parameter r with $\xi_0 = (1 + r)/2$, $\kappa_1 = \kappa_2 = 2$.

Furthermore, by using the parameters used in Figs. 16–21, from Eq. (4.9) we calculate that, respectively

$$(4.12) \quad \frac{R^2 \mu_2 \varepsilon^*}{\sigma^0} = -0.06, 0.1695, -2.7231, 3.9898, -659.7846, 779.8345.$$

We can see from the above that ε^* and σ^0 may have either the same or opposite signs.

5. Conclusions

Using conformal mapping techniques, we demonstrate that neutral coated holes in anti-plane elasticity continue to be available even in the presence of a screw dislocation dipole in the thick coating. A logarithmic function is introduced into the mapping function (3.3) to account for the existence of the screw dislocation dipole. Numerical examples demonstrate the feasibility of the design method. The present method can be easily modified to study the more general case in which the thick coating is under the action of an arbitrary number of screw dislocations with the sum of the Burgers vectors of these dislocations being zero.

Also by means of conformal mapping, we have successfully designed neutral coated holes when a circular thermal inclusion is present in the thick coating and when the matrix is subjected to uniform hydrostatic stresses at infinity. All the unknown coefficients appearing in the mapping function (4.3) are determined quite simply by Eq. (4.5). Numerical results demonstrate the feasibility of our design method. Finally, our results support the conjecture that when a thermal inclusion of *arbitrary* shape is present in the thick coating, the coated hole can still be made neutral to an isotropic field.

Appendix

The continuity conditions of traction and displacement across the perfect circular interface $L_3 : |z - z_0| = R$ can be expressed as follows

$$(A.1) \quad \begin{aligned} \phi_2(z) + z\overline{\phi_2'(z)} + \overline{\psi_2(z)} &= \phi_3(z) + z\overline{\phi_3'(z)} + \overline{\psi_3(z)}, \\ \kappa_2\phi_2(z) - z\overline{\phi_2'(z)} - \overline{\psi_2(z)} &= \kappa_2\phi_3(z) - z\overline{\phi_3'(z)} - \overline{\psi_3(z)} + 2\mu_2\varepsilon^*z, \quad z \in L_3, \end{aligned}$$

where $\phi_3(z)$ and $\psi_3(z)$ are the two complex potentials defined in the circular thermal inclusion whilst $\phi_2(z)$ and $\psi_2(z)$ are the two complex potentials defined in the region occupied by the thick coating outside the circular thermal inclusion, here denoted by S_2' .

After some simple operations, Eq. (A.1) can be rewritten as

$$(A.2) \quad \begin{aligned} \phi_2(z) &= \phi_3(z) + \frac{2\mu_2\varepsilon^*z}{\kappa_2+1}, \\ \psi_2(z) + \frac{4\mu_2\varepsilon^*}{\kappa_2+1} \frac{R^2}{z-z_0} &= \psi_3(z) - \frac{4\mu_2\varepsilon^*\bar{z}_0}{\kappa_2+1}, \quad z \in L_3. \end{aligned}$$

By considering the above, we construct the following two auxiliary functions

$$(A.3) \quad \begin{aligned} \Phi(z) &= \begin{cases} \phi_2(z), & z \in S'_2, \\ \phi_3(z) + \frac{2\mu_2\varepsilon^*z}{\kappa_2+1}, & |z-z_0| \leq R, \end{cases} \\ \Psi(z) &= \begin{cases} \psi_2(z) + \frac{4\mu_2\varepsilon^*}{\kappa_2+1} \frac{R^2}{z-z_0}, & z \in S'_2, \\ \psi_3(z) - \frac{4\mu_2\varepsilon^*\bar{z}_0}{\kappa_2+1}, & |z-z_0| \leq R. \end{cases} \end{aligned}$$

It is seen from Eqs. (A.2) and (A.3) that $\Phi(z)$ and $\Psi(z)$ are continuous across L_3 and then analytic in S_2 , the region occupied by the thick coating.

The definitions in Eq. (A.3) also suggest that the region of definition of the two analytic functions $\phi_2(z)$ and $\psi_2(z)$ can be extended by analytic continuation to the circular domain $|z-z_0| \leq R$ through the following:

$$(A.4) \quad \phi_2(z) = \Phi(z), \quad \psi_2(z) = \Psi(z) - \frac{4\mu_2\varepsilon^*}{\kappa_2+1} \frac{R^2}{z-z_0}, \quad z \in S_2,$$

which indicates that $\phi_2(z)$ is analytic in S_2 whereas $\psi_2(z)$ is meromorphic in S_2 (there is a first-order pole at $z = z_0$).

Equation (4.1c) then follows accordingly. Here we point out that this technique has been adopted by SUO [28]. We can also use the relationship in Eq. (A.3) to arrive at $\phi_3(\xi) = \phi_3(\omega(\xi))$ and $\psi_3(\xi) = \psi_3(\omega(\xi))$ once $\phi_2(\xi)$ and $\psi_2(\xi)$ have been determined.

Acknowledgements

This work is supported by the National Natural Science Foundation of China (Grant No. 11272121) and through the Discovery Grant from the Natural Sciences and Engineering Research Council of Canada (Grant No: RGPIN – 2017 – 03716115112).

References

1. E.H. MANSFIELD, *Neutral holes in plane sheet-reinforced holes which are equivalent to the uncut sheet*, Quarterly Journal of Mechanics and Applied Mathematics, **6**, 371–378, 1953.
2. B. BUDIANSKY, J.W. HUTCHINSON, A.G. EVANS, *On neutral holes in tailored, layered sheets*, ASME Journal of Applied Mechanics, **60**, 1056–1058, 1993.
3. E. SENOCAK, A.M. WAAS, *Neutral holes in laminated plates*, AIAA Journal of Aircraft, **30**, 428–432, 1993.
4. E. SENOCAK, A.M. WAAS, *Neutral cutouts in laminated plates*, Mechanics of Composite Materials and Structures, **2**, 71–89, 1995.

5. C.Q. RU, *Interface design of neutral elastic inclusions*, International Journal of Solids and Structures, **35**, 557–572, 1998.
6. Y. BENVENISTE, T. MILOH, *Neutral inhomogeneities in conduction phenomena*, Journal of the Mechanics and Physics of Solids, **47**, 1873–1892, 1999.
7. R. RICHARDS, *Principles of Solid Mechanics*, CRC Press LLC, USA, 2001.
8. G.W. MILTON, S.K. SERKOV, *Neutral inclusions for conductivity and anti-plane elasticity*, Proceedings of the Royal Society of London A, **457**, 1973–1997, 2001.
9. T. CHEN, Y. BENVENISTE, P.C. CHUANG, *Exact solution in torsion of composite bars: thickly coated neutral inhomogeneities and composite cylinder assemblages*, Proceedings of the Royal Society of London A, **458**, 1719–1959, 2002.
10. P. SCHIAVONE, *Neutrality of an elliptic inhomogeneity in the case of non-uniform loading*, International Journal of Engineering Science, **41**, 2081–2090, 2003.
11. X. WANG, P. SCHIAVONE, *Neutral coated circular inclusions in finite plane elasticity of harmonic materials*, European Journal of Mechanics–A/Solids, **33**, 75–81, 2012.
12. X. WANG, P. SCHIAVONE, *A neutral multi-coated sphere under non-uniform electric field in conductivity*, Journal of Applied Mathematics and Physics (ZAMP), **64**, 895–903, 2013.
13. P. JARCZYK, V. MITYUSHEV, *Neutral coated inclusions of finite conductivity*, Proceedings of the Royal Society of London A, **468**, 2140, 954–970, 2012.
14. M. DAI, P. SCHIAVONE, C.F. GAO, *Neutral nano-inhomogeneities in hyperelastic materials with a hyperelastic interface model*, International Journal of Non-Linear Mechanics, **87**, 38–42, 2016.
15. G.W. MILTON, M. BRIANE, J.R. WILLIS, *On cloaking for elasticity and physical equations with a transformation invariant form*, New Journal of Physics, **8**, 10, 248, 2006.
16. L.P. LIU, *Neutral shells and their applications in the design of electromagnetic shields*, Proceedings of the Royal Society of London A, **466**, 3659–3677, 2010.
17. H. AMMARI, H. KANG, H. LEE, M. LIM, *Enhancement of near cloaking using generalized polarization tensors vanishing structures. Part I: The conductivity problem*, Communications in Mathematical Physics, **317**, 1, 253–266, 2013.
18. G.I. TAYLOR, *The mechanism of plastic deformation of crystals. Part I, Theoretical*, Proceedings of the Royal Society A, **145**, 362–387, 1934.
19. T. MURA, *Continuous distribution of dislocations and the mathematical theory of plasticity*, Physica Status Solidi, **10**, 447–453, 1965.
20. T. MURA, *Continuum theory of plasticity and dislocations*, International Journal of Engineering Science, **5**, 341–351, 1967.
21. I. GROMA, *Link between the microscopic and mesoscopic length-scale description of the collective behavior of dislocations*, Physical Review B, **56**, 5807–5813, 1997.
22. V. VINOGRADOV, J.R. WILLIS, *The pair distribution function for an array of screw dislocations*, International Journal of Solids and Structures, **45**, 3726–3738, 2008.
23. V. VINOGRADOV, J.R. WILLIS, *The pair distribution function for an array of screw dislocations: implications for gradient plasticity*, Mathematics and Mechanics of Solids, **14**, 161–178, 2009.

-
24. T.C.T. TING, *Anisotropic Elasticity—Theory and Applications*, Oxford University Press, New York, 1996.
 25. N.I. MUSKHELISHVILI, *Some Basic Problems of the Mathematical Theory of Elasticity*, P. Noordhoff Ltd., Groningen, 1953.
 26. G.W. MILTON, *Bounds on the complex dielectric constant of a composite material*, Applied Physics Letters, **37**, 300–302, 1980.
 27. G.W. MILTON, *Bounds on the complex permittivity of a two-component composite material*, Journal of Applied Physics, **52**, 5286–5293, 1981.
 28. Z.G. SUO, *Singularities interacting with interfaces and cracks*, International Journal of Solids and Structures, **25**, 1133–1142, 1989.
 29. C.Q. RU, *Analytic solution for Eshelby’s problem of an inclusion of arbitrary shape in a plane or half-plane*, ASME Journal of Applied Mechanics, **66**, 315–322, 1999.
 30. G.P. CHEREPANOV, *Inverse problem of the plane theory of elasticity*, Prikladnaya Matematika Mechanika (PMM), **38**, 963–979, 1974.

Received May 22, 2018; revised version September 29, 2018.
